

# Discrete Symmetries and $\frac{1}{3}$ -Quantum Vortices in Condensates of $F = 2$ Cold Atoms

Gordon W. Semenoff and Fei Zhou

*Department of Physics and Astronomy, The University of British Columbia, Vancouver, B.C., Canada V6T 1Z1*

(Dated: June 11, 2018)

In this Letter we study discrete symmetries of mean field manifolds of condensates of  $F = 2$  cold atoms, and various unconventional quantum vortices. Discrete quaternion symmetries result in two species of spin defects that can only appear in integer vortices while *cyclic* symmetries are found to result in a phase shift of  $2\pi/3$  (or  $4\pi/3$ ) and therefore  $1/3$ - (or  $2/3$ -) quantum vortices in condensates. We also briefly discuss  $1/3$ -quantum vortices in condensates of trimers.

One of the most striking features of a superfluid is the existence of quantized vortices. This is a consequence of the requirement that the quantum mechanical wavefunction of any physical state be single-valued. In a standard single component bosonic condensate, this requirement results in the quantization of circulation: the line-integral of the superfluid velocity along a path linking a vortex takes discrete values:  $\oint d\mathbf{r} \cdot \mathbf{v}_s = n \cdot \frac{2\pi\hbar}{m}$ , with  $n$  an integer. Here,  $\frac{2\pi\hbar}{m}$  is the fundamental quantum of circulation. The quantization of circulation has been observed in superfluid liquid Helium by Vinen [1], and recently in Bose-Einstein condensates of cold atoms [2]; the presence of quantized vortices usually results in discrete values in the energy splitting of collective modes that have been studied in experiments.

The existence of quantized vortices in a condensate is also tied to the topology of the vacuum manifold. In a single component condensate, the vacuum manifold is the set of all distinct phases that the condensate can have. This set is identical to the unit circle  $S^1$ . As one moves in a closed path around a quantized vortex, the phase must traverse  $S^1$  an integer number of times [3, 4, 5, 6]. For condensates with more than one component, vortices can have circulation quantized as fractions of the basic unit  $\frac{2\pi\hbar}{m}$ ; this is achieved when a change of phase is combined with a rotation of spin or orbital orientation. A most recent example are the half-quantum vortices in condensates of sodium atoms[7]; half vortices were also discussed in the context of superfluid  ${}^3\text{He}$ [4].

Cold atoms in optical traps and lattices are a promising venue where exotic condensates and vortices could be realized in nature. Spin correlated states of spin  $F = 1$  cold atoms have already been explored experimentally [8] and theoretically [9, 10, 11]. More recently, the scattering lengths of spin  $F = 2$  cold atoms have also been investigated [12] and various possible condensates have been pointed out [13, 14]. In this letter we shall examine the possible appearance of unconventional vortices in the latter condensates. In a previous study of their possible insulating phases [15], we found a convenient parametrization of the  $F = 2$  wave-function as a tensor  $\chi_{\alpha\beta}$  where  $\alpha, \beta$  take the values  $x, y, z$ . Being the wave-function of an atom, the entries of this matrix are complex functions. To be a state with  $F = 2$ , it must be symmetric,

$\chi_{\alpha\beta} = \chi_{\beta\alpha}$ , and traceless,  $\text{tr}\chi = \chi_{xx} + \chi_{yy} + \chi_{zz} = 0$ . This leaves five independent complex entries. These entries are linear combinations of the five components of the atom wave-function  $\psi_{m_F}$  with  $m_F = 2, 1, 0, -1, -2$  the  $z$ -component of the spin. In Ref. [15], we related the Landau-Ginzburg free energy functional of the condensate to recently measured scattering lengths for atoms. By including a derivative term, in the long-wavelength limit we have

$$\mathcal{E} = \int d\mathbf{r} \rho_0 \left[ \frac{\hbar^2}{m^*} \text{tr} \nabla \chi^*(\mathbf{r}) \cdot \nabla \chi(\mathbf{r}) + MA(\chi(\mathbf{r}), \chi^*(\mathbf{r})) \right],$$

$$A(\chi, \chi^*) = 4b_L \text{Tr}[\chi, \chi^*]^2 + 2c_L \text{tr} \chi^2 \text{Tr} \chi^{*2} \quad (1)$$

$m^*$  is the effective mass of atoms in optical lattices,  $M$  is the average number of atoms per site and  $\rho_0$  the average particle density. The coefficients  $b_L$  and  $c_L$  can be estimated from the two-atom interaction strengths in channels with various spins[15];  $b_L$  or  $c_L$  is proportional to  $b = (a_4 - a_2)/7$  or  $c = (a_0 - a_4)/5 - 2(a_2 - a_4)/7$  and  $a_{0,2,4}$  are two-body  $s$ -wave scattering lengths in  $F = 0, 2, 4$  channels respectively. For ground states we consider uniform condensates. The  $\chi$ -dependence of the energy of condensates is identical to that of Mott states obtained earlier in Ref.[15]; minimization of this energy subject to a constraint of  $\text{tr} \chi^* \chi = 1/2$  was previously carried out.

When all scattering lengths are equal,  $A(\chi, \chi^*) = 0$  and the Hamiltonian is  $SU(5)$  symmetric. The mean field manifold is  $U(1) \times SU(5)$ .  $SU(5)$  is simply connected and its fundamental group is trivial. Only integer vortices are allowed in this case. Restoring the spin-dependent scattering turns on the potential and, as shown below, results in multiply connected mean field manifolds and exotic vortices. Here we investigate various discrete symmetries of the manifolds for cyclic and nematic phases.

When  $b_L > 0$ , and  $c_L > 0$ , the energy is minimized by a ground state  $\chi$  satisfying  $\text{tr} \chi^2 = 0 = [\chi, \chi^*]$ . The real and imaginary parts of  $\chi$  commute with each other and we can find a coordinate frame where  $\chi$  is diagonal. A solution which obeys  $\text{tr} \chi = 0$  as well as  $\text{tr} \chi^* \chi = \frac{1}{2}$  is

$$\chi_+ = \frac{1}{\sqrt{6}} \begin{bmatrix} 1 & 0 & 0 \\ 0 & \omega & 0 \\ 0 & 0 & \omega^2 \end{bmatrix}, \quad \omega = e^{i2\pi/3} \quad (2)$$

The full set of degenerate solutions can be obtained by applying symmetry transformations:  $SO(3)$  rotations, implemented by  $3 \times 3$  orthogonal matrices  $\mathcal{R}$  and multiplication by a  $U(1)$  phase,  $e^{i\xi}$ , to the solution  $\chi_+$ . An arbitrary solution  $\chi$  can be written as  $e^{i\xi}\mathcal{R}\chi_+\mathcal{R}^{-1}$ .

The set of all solutions is equal to the group of all such symmetry transformations factored by the subgroup which leaves  $\chi_+$  invariant. As we shall explain below, this subgroup is the tetrahedral group,  $T$ . The vacuum manifold is therefore the set of right cosets  $\mathcal{M} = \frac{SO(3) \times U(1)}{T}$  [16]. The tetrahedral group,  $T$ , is the subgroup of  $SO(3) \times U(1)$  which leaves  $\chi_+$  in eq. (2) invariant. This group contains the identity, and three diagonal  $SO(3)$  matrices (called the Klein 4-group)

$$\mathbf{1} = \begin{pmatrix} 1 & 0 & 0 \\ 0 & 1 & 0 \\ 0 & 0 & 1 \end{pmatrix}, \quad \mathcal{I}_x = \begin{pmatrix} 1 & 0 & 0 \\ 0 & -1 & 0 \\ 0 & 0 & -1 \end{pmatrix}$$

$$\mathcal{I}_y = \begin{pmatrix} -1 & 0 & 0 \\ 0 & 1 & 0 \\ 0 & 0 & -1 \end{pmatrix}, \quad \mathcal{I}_z = \begin{pmatrix} -1 & 0 & 0 \\ 0 & -1 & 0 \\ 0 & 0 & 1 \end{pmatrix}. \quad (3)$$

The remaining elements of  $T$  implement cyclic permutations of the diagonal elements of  $\chi_+$  as well as multiplication by phases. The the elements of  $SO(3)$  which permute the diagonal elements of  $\chi_+$  are

$$\mathcal{C} = \begin{pmatrix} 0 & 0 & 1 \\ 1 & 0 & 0 \\ 0 & 1 & 0 \end{pmatrix}, \quad \mathcal{C}^2 = \begin{pmatrix} 0 & 1 & 0 \\ 0 & 0 & 1 \\ 1 & 0 & 0 \end{pmatrix} \quad (4)$$

Indeed,  $\chi_+ = \omega\mathcal{C}\chi_+\mathcal{C}^{-1}$ , where  $\omega$  was introduced in Eq. (2). The elements  $\mathbf{1}, \mathcal{C}, \mathcal{C}^2$  form a cyclic subgroup of  $SO(3)$ ,  $C_3$ . We emphasize that the transformation of  $\chi_+$  involves a  $U(1)$  phase of  $\frac{2\pi}{3}$  as well as a cyclic rotation represented by  $\mathcal{C}$ . We will denote this combination of transformations as  $\tilde{\mathcal{C}}$ . The full tetrahedral group  $T$  has the 12 elements  $T = \{\mathbf{1}, \mathcal{I}_x, \mathcal{I}_y, \mathcal{I}_z, \tilde{\mathcal{C}}, \mathcal{I}_x\tilde{\mathcal{C}}, \mathcal{I}_y\tilde{\mathcal{C}}, \mathcal{I}_z\tilde{\mathcal{C}}, \tilde{\mathcal{C}}^2, \mathcal{I}_x\tilde{\mathcal{C}}^2, \mathcal{I}_y\tilde{\mathcal{C}}^2, \mathcal{I}_z\tilde{\mathcal{C}}^2\}$ .

The first step in classifying vortices is to identify the homotopy group  $\Pi_1(\mathcal{M})$  [17]. Since  $SO(3)$  is not simply connected, to understand the topology of the manifold  $\mathcal{M}$  we shall lift  $SO(3)$  to  $SU(2)$ . An element of  $SU(2)$  is a  $2 \times 2$  unitary matrix. The set of  $2 \times 2$  unitary matrices is characterized by the four real Euler parameters ( $e_0, \mathbf{e}$ ) through the relation  $\mathbf{Q} = e_0 + i\mathbf{e} \cdot \vec{\sigma}$ ;  $\vec{\sigma}$  are the usual Pauli matrices.  $\mathbf{Q}$  is unitary when  $e_0^2 + \mathbf{e} \cdot \mathbf{e} = 1$ ; the Euler parameters live on the unit three-sphere  $S^3$ , which is simply connected. The matrix  $\mathbf{Q}$  is the well-known quaternion representation of a rotation [18]. The  $3 \times 3$  rotation matrix  $\mathcal{R} \in SO(3)$  which corresponds to  $\mathbf{Q} \in SU(2)$  is  $\mathcal{R}_{\alpha\beta} = \frac{1}{2}\text{Tr}(\sigma_\alpha\mathbf{Q}\sigma_\beta\mathbf{Q}^\dagger)$ . This is a two-to-one mapping since both  $\mathbf{Q}$  and  $-\mathbf{Q}$  are mapped to the same  $\mathcal{R}$ . The inverse,  $\mathcal{R} \rightarrow (\mathbf{Q}, -\mathbf{Q})$  is the ‘lift’ of  $\mathcal{R}$  to  $SU(2)$ .

We also need to lift the tetrahedral group  $T$  to  $T^*$ , the binary tetrahedral group which is a subgroup of  $SU(2)$

and contains 24 elements. For this, we must identify the pair of  $SU(2)$  matrices which correspond to each of the 12 elements of  $T$ . The elements of  $T$  are the simple rotations (examples are shown in Fig.2) that lift as:  $\mathbf{1} \rightarrow \pm\mathbf{1}$ ,  $\mathcal{I}_{x,y,z} \rightarrow \pm i\sigma_{x,y,z}$ ,  $\mathcal{C} \rightarrow \pm\sigma = \pm\frac{1}{2}(1 + i\sigma_x + i\sigma_y + i\sigma_z)$ . We further denote a rotation  $\sigma$  combined with a phase shift of  $2\pi/3$  as  $\tilde{\sigma}$ . The group elements of  $T^*$  which are lifts of  $T$  are therefore,

$$\pm i\sigma_x, \pm i\sigma_y, \pm i\sigma_z, \pm\mathbf{1} \quad (5)$$

$$\pm i\sigma_x\tilde{\sigma}, \pm i\sigma_y\tilde{\sigma}, \pm i\sigma_z\tilde{\sigma}, \pm\tilde{\sigma} \quad (6)$$

$$\pm i\sigma_x\tilde{\sigma}^2, \pm i\sigma_y\tilde{\sigma}^2, \pm i\sigma_z\tilde{\sigma}^2, \pm\tilde{\sigma}^2. \quad (7)$$

Eq.(5) represents the quaternion subgroup  $Q$ .

The vacuum manifold derived above is isomorphic to

$$\mathcal{M} = \frac{SU(2) \times U(1)}{T^*}. \quad (8)$$

To find the homotopy classes of closed paths in  $\mathcal{M}$ , we must first understand how they are related to paths in the product of space of  $SU(2) \times U(1)$ . As we have discussed above,  $SU(2)$  is equivalent to a three-sphere  $S^3$ , and  $U(1)$  to a circle  $S^1$ , so that we could equivalently think of paths on the product space  $S^3 \times S^1$ . Each point of  $S^3 \times S^1$  corresponds to an element in the group  $SU(2) \times U(1)$ . Factoring by  $T^*$  is simply making an identification on  $S^3 \times S^1$ , each point is to be identified with 23 other points which are obtained from the corresponding group element by operation of the non-trivial elements of  $T^*$ .

Consider a path on  $S^3 \times S^1$ . In order to be a closed path on  $\mathcal{M}$  it must either end at the point on  $S^3 \times S^1$  at which it began, or it must end at one of 23 points that are identified with it. As shown in Fig. 1, there are three types of paths (which all begin at the identity):

**Type A:** Paths that traverse  $S^1$   $n$  ( $n$  is an integer) times and end with one of the eight elements in Eq.(5);

**Type B:** Paths that traverse  $S^1$   $n + \frac{1}{3}$  times and end with one of eight elements in Eq.(6);

**Type C:** Paths that traverse  $S^1$   $n + \frac{2}{3}$  times and end with one of eight elements in Eq.(7).

Thus each path is characterized with two variables: the winding number around  $S^1$  and an element in  $T^*$ .  $\Pi_1(\mathcal{M}) = \{(n, \mathbf{1}), (n, -\mathbf{1}), (n, i\sigma_\alpha), (n, -i\sigma_\alpha), (n + \frac{1}{3}, \tilde{\sigma}), (n + \frac{1}{3}, -\tilde{\sigma}), (n + \frac{1}{3}, i\sigma_\alpha\tilde{\sigma}), (n + \frac{1}{3}, -i\sigma_\alpha\tilde{\sigma}), (n + \frac{2}{3}, \tilde{\sigma}^2), (n + \frac{2}{3}, -\tilde{\sigma}^2), (n + \frac{2}{3}, i\sigma_\alpha\tilde{\sigma}^2), (n + \frac{2}{3}, -i\sigma_\alpha\tilde{\sigma}^2)\}$ . This set forms an infinite order non-abelian discrete group with composition law  $(x, g_1) \cdot (y, g_2) = (x + y, g_1g_2)$ .

So far, we have computed the homotopy group  $\Pi_1(\mathcal{M})$  for loops with a base-point. However, distinct vortices are identified with free homotopy classes, which coincide with conjugacy classes of the based homotopy group [4, 5]. For an element  $g_i$  of a group, the conjugacy class is the set of all distinct elements in the set  $g_ag_g^{-1}$  as  $g_a$  sweeps over the group. In our case, the classes are 1)  $\{(n, \mathbf{1})\}$ ; 2)  $\{(n, -\mathbf{1})\}$ ; 3)  $\{(n, i\sigma_\alpha), (n, -i\sigma_\alpha)\}$ ,  $\alpha =$

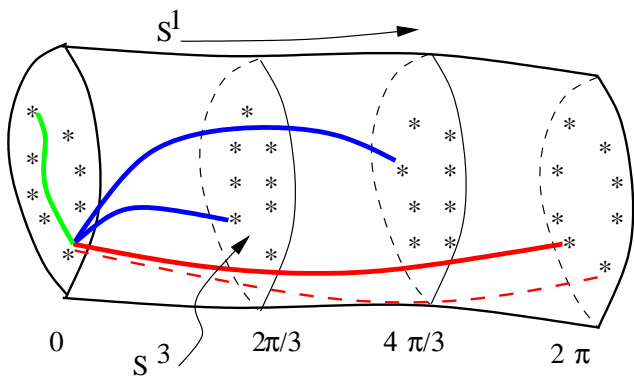


FIG. 1: (color online) Schematic of the mean field manifold of cyclic condensates. The unit circle is oriented horizontally with phase angles  $\xi$  (defined after Eq.2) around it shown explicitly. Each cross section at a given angle stands for a three-sphere. Examples of 24 four identified points in the product space  $S^3 \times S^1$  are shown explicitly as stars, with eight points at  $\xi = 0$  or  $2\pi$  (or elements in Eq.5), eight points at  $\xi = 2\pi/3$  (or elements in Eq.6), and the eight points at  $\xi = 4\pi/3$  (or elements in Eq.7). The red path ending at phase  $2\pi$  is for an integer vortex with a spin defect inserted; the red dashed one is for a plain integer vortex without spin defects. The short (long) blue path ending at  $2\pi/3$  ( $4\pi/3$ ) is for a  $1/3$  ( $2/3$ )-quantum vortex. The green path at phase  $\xi = 0$  corresponds to a spin defect and the winding along  $S^1$  is trivial.

$x, y, z$ ; 4)  $\{(n + \frac{1}{3}, \tilde{\sigma}), (n + \frac{1}{3}, -i\sigma_\alpha \tilde{\sigma})\}$ ; 5)  $\{(n + \frac{1}{3}, -\tilde{\sigma}), (n + \frac{1}{3}, i\sigma_\alpha \tilde{\sigma})\}$ ; 6)  $\{(n + \frac{2}{3}, \tilde{\sigma}^2), (n + \frac{2}{3}, -i\sigma_\alpha \tilde{\sigma}^2)\}$ ; 7)  $\{(n + \frac{2}{3}, -\tilde{\sigma}^2), (n + \frac{2}{3}, i\sigma_\alpha \tilde{\sigma}^2)\}$ . Altogether there are *only* seven distinct classes and thus seven types of linear defects.

If  $n = 0$ , a Type-A path corresponds to a pure spin vortex. Such a path might begin at the origin (identity) and end at one of  $\pm i\sigma_x, \pm i\sigma_y, \pm i\sigma_z$  or  $-\mathbf{1}$ . These correspond to, respectively,  $180^\circ$  rotations around one of the three axes  $\hat{x}, \hat{y}, \hat{z}$  or a rotation around the  $\hat{z}$ -axis by  $360^\circ$  (see (b-e) in Fig. (2)). However, paths which end at  $\pm i\sigma_x, \pm i\sigma_y, \pm i\sigma_z$  are freely homotopic to each other and all represent the same spin defect. So there are two differ types of spin vortices (specified by classes):  $(0, -\mathbf{1})$  and  $(0, \pm i\sigma_\alpha)$ ,  $\alpha = x, y$  or  $z$ .

On the other hand when  $n$  is a nonzero integer, a type-A path corresponds to an integer vortex. Three conjugacy classes involving integer  $n$  represent *three* distinct species of integer vortices: a conventional integer vortex with no spin structure, an integer vortex with a spin defect of  $(0, -\mathbf{1})$  inserted and an integer vortex with a spin defect of  $(0, \pm i\sigma_\alpha)$  inserted. The last two types are unique to condensates of  $F = 2$  atoms.

Along Type-B or Type-C paths, a phase shift of  $2\pi/3$  or  $4\pi/3$  is generated under the action of the element  $\tilde{\sigma}_c$  or  $\tilde{\sigma}_c^2$ . In these cases, the spin rotation leads to a  $1/3$ -quantum vortex or a  $2/3$ -quantum vortex. Furthermore, there are only two topologically distinct species of each of  $1/3$ - or  $2/3$ -vortices. The two distinct  $1/3$ -quantum

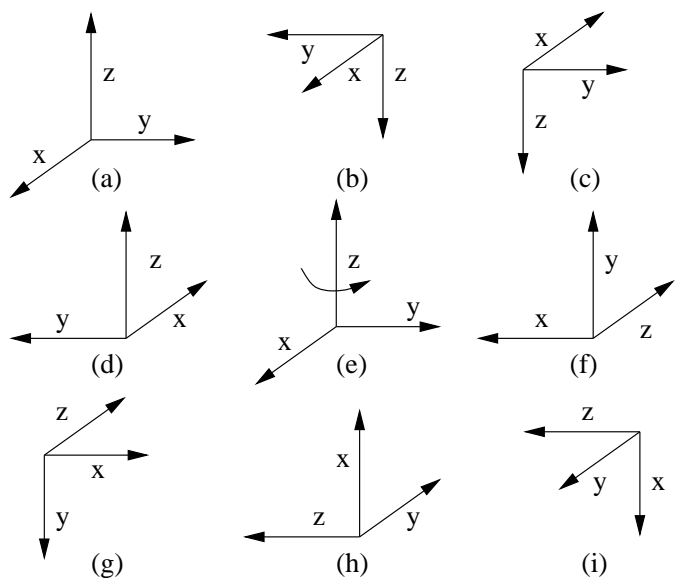


FIG. 2: Spin rotations in integer vortices,  $1/3$ -quantum vortices and  $2/3$ -quantum vortices. (a) the orientation of three basis vectors  $\hat{x}\hat{y}\hat{z}$  at azimuthal angle  $\phi = 0$ . (b-e) the orientation of the triad  $\hat{x}\hat{y}\hat{z}$  at angle  $\phi = 2\pi$  in four configurations of integer vortices:  $(0, i\sigma_x)$  (b),  $(0, i\sigma_y)$  (c),  $(0, i\sigma_z)$  (d),  $(0, -\mathbf{1})$  (e); the arrow in (e) represents a  $360^\circ$  rotation around the  $z$  axis. (f,g) the orientation of the triad  $\hat{x}\hat{y}\hat{z}$  at angle  $\phi = 2\pi$  in two  $1/3$  quantum vortices:  $(1/3, i\sigma_z\tilde{\sigma})$  (f),  $(1/3, i\sigma_y\tilde{\sigma})$  (g); (h,i) the orientation of the triad  $\hat{x}\hat{y}\hat{z}$  at angle  $\phi = 2\pi$  in two  $2/3$  quantum vortices:  $(2/3, i\sigma_z\tilde{\sigma}^2)$  (h),  $(2/3, i\sigma_x\tilde{\sigma}^2)$  (i).

vortices are represented by either paths that end with elements  $\tilde{\sigma}, -i\sigma_\alpha \tilde{\sigma}$  or paths that end with  $-\tilde{\sigma}, i\sigma_\alpha \tilde{\sigma}$ . The  $1/3$  and  $2/3$ -quantum vortices necessarily contain topologically non-trivial spin configurations which differ in structure from those in integer vortices.

We now are going to examine spatially slowly varying matrix  $\chi(\mathbf{r})$  and focus on spin vortices and  $1/3$ -quantum vortices. All linear defects are oriented along the  $z$ -direction; the center of a defect is at the origin of cylindrical coordinates  $(\rho, \phi, z)$ . The superfluid velocity in the condensate is  $\mathbf{v}_s = 2\text{Im} \text{tr} \chi^* \nabla \chi \hbar/m$ . Far away from the center, the wavefunction of a pure spin vortex is specified by the rotation,  $\chi(\rho = +\infty, \phi) = \mathcal{R}(\phi)\chi_+\mathcal{R}^T(\phi)$ . To minimize the energy in Eq.(1), we find that the rotation matrix satisfies the equation

$$[\chi_+, \frac{\partial A}{\partial \phi}] = 0, \text{ where } A = \mathcal{R}^T \frac{\partial \mathcal{R}}{\partial \phi}. \quad (9)$$

A solution can be expressed as  $\mathcal{R}(\phi) = \exp(in \cdot \mathbf{L}f(\phi))$ , where  $f(\phi)$  is a *linear* function of  $\phi$ . Alternatively

$$\mathcal{R}_{\alpha\beta}(\phi) = \delta_{\alpha\beta} \cos f(\phi) + \sin f(\phi) \epsilon_{\alpha\beta\gamma} n_\gamma + n_\alpha n_\beta (1 - \cos f(\phi)). \quad (10)$$

Here  $\mathbf{L}$  is a matrix vector,  $L_{\beta\gamma}^\alpha = -i\epsilon_{\alpha\beta\gamma}$ ,  $\epsilon_{\alpha\beta\gamma}$  is the antisymmetric tensor.  $\mathbf{n}$  is a unit vector with three com-

ponents  $n_\alpha$ ,  $\alpha = x, y, z$ . For a configuration that is specified by the boundary condition:  $\mathcal{R}(0) = 1, \mathcal{R}(2\pi) = \mathcal{I}_z$ , we find the following solution

$$f(\phi) = \frac{\phi}{2}, \mathbf{n} = \mathbf{e}_z. \quad (11)$$

The superfluid velocity is zero. When going around this vortex, the local triad of three orthogonal basis vectors  $\hat{x}\hat{y}\hat{z}$  makes a 180 rotation around  $\hat{z}$ -axis (see Fig.(2d) ).

In a 1/3-quantum vortex, the boundary condition is  $\mathcal{R}(\phi = 0) = 1, \mathcal{R}(\phi = 2\pi) = \mathcal{I}_z \mathcal{C}$ ; at any  $\phi$ ,  $\chi(\phi) = e^{i\phi/3} \mathcal{R}(\phi) \chi_+ \mathcal{R}^T(\phi)$ . The solution which satisfies Eq.(9) and boundary conditions is

$$f(\phi) = \frac{\phi}{3}, \mathbf{n} = \frac{1}{\sqrt{3}}(-\mathbf{e}_x + \mathbf{e}_y - \mathbf{e}_z). \quad (12)$$

One can calculate the circulation integral and confirm that  $\oint \mathbf{dr} \cdot \mathbf{v}_s = \frac{1}{3} \frac{2\pi\hbar}{m}$ . A 1/3-quantum vortex is always superimposed with a *spin* defect and is a unique composite excitation in coherent condensates. When going around this vortex, effectively the local triad  $\hat{x}\hat{y}\hat{z}$  is permuted cyclically:  $\hat{x}\hat{y}\hat{z} \rightarrow \hat{y}\hat{z}\hat{x}$ ; this is accompanied by a  $180^\circ$  rotation around the  $\hat{y}$  axis (see Fig.(2f)). The stability can be studied by examining the core structure. Similar discussions were presented for half-vortices [19].

When  $b_L > \frac{c_L}{4}$  and  $c_L < 0$ ,  $\chi$  satisfies  $\text{tr}\chi^2 = 1/2, \chi = \chi^*$  which corresponds to biaxial nematics [15]. A *real* solution is again invariant under the subgroup in Eq.(3); the submanifold should be isomorphic to  $\mathcal{M}_n = \frac{S^3}{Q} \times S^1$ ,  $Q$  is the quaternion group introduced before[20]. There are quaternion spin defects but *no* 1/3-quantum vortices in this case. The quaternion vortices are analogous to disclinations in cholesteric liquid crystals [4, 5, 6, 21].

In conclusion, we have studied discrete symmetries in condensates of  $F = 2$  cold atoms and investigated 1/3-quantum vortices and pure spin defects. It is worth remarking that 1/3-quantum vortices are also natural topological excitations in condensates of singlets of three atoms (an analogue of Cooper pairs in a two-body channel) or condensates of trimers. Rotationally invariant Mott states of trimers were pointed out by the authors recently[15]. If a trimer condensate does exist in optical lattices (say created by removing atoms from a trimer Mott state), there will then be simple 1/3-quantum vortices that are *featureless* in the spin subspace. Note

that 1/3-quantum vortices in a cyclic phase on the other hand have very rich spin structure as discussed above. The one-third circulation quantum can be studied by observing fractionalized values in the energy splitting of collective modes in experiments similar to those in Ref.[1, 2]. FZ is in part supported by the office of the Dean of Science at the University of British Columbia, NSERC (Canada), Canadian Institute for Advanced Research and the Alfred P. Sloan foundation.

- 
- [1] W. F. Vinen, Nature **181**, 1524 (1958).
  - [2] F. Chevy, K. W. Madison and J. Dalibard, Phys. Rev. Lett. **85**, 2223 (2000); F. Chevy *et al.*, Phys. Rev. A **64**, 031601 (2001).
  - [3] G. Toulouse and M. Kleman, J. Phys. Lett. (Paris)**37**, L149 (1976).
  - [4] G. E. Volovik and V. P. Mineev, Sov. Phys. JETP **45**, 1186 (1977).
  - [5] N. D. Mermin, Rev. Mod. Phys. **51**, 591 (1979).
  - [6] D. J. Thouless, *Topological Quantum Numbers in Non-relativistic Physics* (World Scientific, 1988).
  - [7] F. Zhou, Phys. Rev. Lett. **87**, 080401 (2001); F. Zhou and M. Snoek, Ann. Phys. (N.Y.) **308**, 692 (2003).
  - [8] D. M. Stamper-Kurn *et al.*, Phys. Rev. Lett. **80**, 2027 (1998); J. Stenger *et al.*, Nature **396**, 345 (1998).
  - [9] T. L. Ho, Phys. Rev. Lett. **81**, 742 (1998); T. Ohmi and K. Machida, J. Phys. Soc. Jpn. **67**, 1822 (1998).
  - [10] E. Demler, F. Zhou, Phys. Rev. Lett. **88**, 163001 (2002).
  - [11] S. Mukerjee *et al.*, Phys. Rev. Lett. **97**, 120406 (2006).
  - [12] A. Widera *et al.*, New. J. Phys. **8**, 152 (2006); also J. L. Roberts *et al.*, Phys. Rev. Lett. **81**, 5109 (1998); N. Klausen *et al.*, Phys. Rev. A **64**, 053602 (2001).
  - [13] C. V. Ciobanu *et al.*, Phys. Rev. A **61**, 033607 (2000).
  - [14] M. Koashi, M. Ueda, Phys. Rev. Lett. **84**, 1066 (2000).
  - [15] F. Zhou and G. W. Semenoff, Phys. Rev. Lett. **97**, 180411 (2006).
  - [16] For Mott states, the manifold can be identified as  $SO(3)/T$  that is consistent with a result in R. Barnett *et al.*, Phys. Rev. Lett. **97**, 180412 (2006).
  - [17] A somewhat different approach can be found in H. Makela *et al.*, J. Phys. A: Math. Gen. **36**, 8555 (2003).
  - [18] H. Goldstein, *Classical Mechanics* (Addison Wesley, 1980), Chapter 4.
  - [19] J. Ruostekoski and J. R. Anglin, Phys. Rev. Lett. **91**, 190402 (2003).
  - [20] Here we exclude solutions with special symmetries.
  - [21] M. Kleman, and J. Friedel, J. Phys. (Paris) **30**, Suppl. C4, 43 (1969).